Model-Free Building Temperature Control and Power Allocation Under Measurement Time Delays

Bhagyashri Telsang, University of Tennessee Knoxville
Seddik Djouadi, University of Tennessee Knoxville
Mohammed Olama, Oak Ridge National Laboratory

ABSTRACT

Taking a step towards a greener planet has created an increased need for a higher integration of renewable energy resources into the electric grid. Nonetheless, the intermittency and uncertainty associated with renewable generation have slowed down this integration. Transactive control (TC) has been recently adopted to address this challenge by utilizing demand side flexibility and enabling the participation of many grid-interactive efficient buildings (GEBs). However, existing TC methods require significant modeling and/or training efforts and are computationally expensive. To address the aforementioned issues, we propose a model-free control (MFC)-based strategy that is robust to the time delays in the temperature measurements of the thermostatically controlled loads (TCLs). It assigns to each GEB a local controller to maintain the TCLs' temperatures within desired comfort levels, while the load aggregator (LA) allocates the assigned reference power provided by the distribution system operator (DSO) to support a specific grid service, such as demand peak reduction, load shifting, balancing supply and demand, and consuming the solar photovoltaic power locally. We investigate the effects of such loss of information on the local control action as well as on meeting the power allocation constraint. We conclude that, for an appropriate choice of design parameters, the proposed MFC controller is satisfactorily robust to measurement time delays.

Introduction

Either stemming from the need to reduce carbon emissions or to geopolitically insulate the local markets, the need for integration of renewable energy in the electrical mainframe and day-to-day consumption has been on the rise. Research in the area has responded through different lines of development – demand-response (DR) strategies, peer-to-peer electricity sharing, dynamic electricity pricing, and others (Park, 2017). However, as more components get added on, the chance of failure of the overall system also increases. This causes a need to proactively look ahead and build fault tolerance and robustness in the systems to increase their overall reliability.

The existing literature on the fault tolerance of control systems in microgrids is reviewed in Ortiz (2020). To dynamically balance the loads, time delays are included in the system models in Hayat et al. (2003). A detailed study on time delays in real systems and ways to handle them is presented in Nilsson (1998). These works require accurate system models of the different building loads that is hard to obtain in practice.

In this paper, we choose a model-free control (MFC) strategy developed in Fliess (2014) to maintain the desired load output and analyze its robustness to time delays. The said data-driven strategy has been widely employed in a range of real applications (Jama et al. 2017; Lafont et al. 2015; MohammadRidha et al. 2017). Its inherent ability to adaptively estimate the to-be-controlled-system in real-time also allows it to handle various attributes like system nonlinearities and time delays.

In Telsang et al. (2018), an MFC strategy to allocate a certain reference power profile among a group of building thermostatically controlled loads (TCLs) has been investigated. Such a reference power profile could either be generated from a solar energy source, or it could be obtained as a result of a DR strategy that a load aggregator (LA) is supposed to manage among the participating loads. In either case, there is a central command center that receives the input power consumption of the participating TCLs and their corresponding temperature measurements for all the TCLs. Based on the received information and the available power at that time instant, the central command center communicates back to each local controller the input power to each TCL such that the power allocation constraint is satisfied. In Telsang et al. (2021), the case where there are different importance levels for different load types has been considered and a weighted power allocation strategy through projection has been developed. Additionally, in the same work, the feasibility of a reference power profile has been investigated.

In this paper, we consider practical issues and investigate the situation where there is a measurement defect on the local side. Specifically, if there is a fault in the local measurement system and the TCL temperature output is measured with a time-delay, then the time lag is reflected in the measurement communicated from the local controller to the central command center as well. We investigate the performance of the proposed MFC strategy and its integration in the power allocation scheme under existence of measurement time delays. That is, we investigate the robustness of the local control method against such measurement time delays as well as the effect of such time delays on satisfying the power allocation constraint by the central command center.

The paper is structured as follows. First, we briefly review the MFC strategy employed on the local control action, followed by a description of the Heating, Ventilation, and Air Conditioning (HVAC) models used in this study. Then, we investigate the indoor air temperatures resulting from controlling the HVACs with and without introducing time delays in the measurements. We compare the performance of MFC with a simple thermostat control that turns the HVAC on or off in response to the measured air temperature. Following the analysis on the local side, we then present the central algorithm that performs power allocation and study its performance in the presence of measurement time delays. Finally, we conclude with some remarks and future work.

Overview of MFC

A SISO system is approximated by the following ultra-local model (Fliess, 2014):

$$\dot{y} = F + \alpha u$$

Here, F represents the uncertainties in the system at that time, and α is a tuning parameter to match the magnitudes of the input and the derivative of the output. Using previous L seconds of input and output measurements, F is approximated as ϕ (Fliess, 2014):

$$F \approx \phi = \frac{-6}{L^3} \int_{t-L}^{t} (L - 2\sigma) y(\sigma) + \alpha\sigma(L - \sigma) u(\sigma) d\sigma$$

Using the latest approximation of the system, the control input is computed as (Fliess, 2014):

$$u = -\frac{F - \dot{y}^* + K_p(y - y^*)}{\alpha}$$

Here, K_p is the proportional control gain and $\dot{y}^*$ is the derivative of the desired trajectory y^*.

The tuning parameters in MFC are α and L.

In this paper, we analyze MFC for its effectiveness and robustness against time delays in measurements. To do so, we consider twenty different first-order models to represent a range of HVAC systems and control them using the MFC to maintain the indoor air temperature at a desired setpoint.

HVAC Models

We consider the following first-order state-space model to represent the cooling of indoor spaces by HVAC:

$$x(k+1) = Ax(k) + B\,u(k) + G\,v(k)$$
$$y(k) = C\,x(k) + Du(k)$$

The system matrices are given as:

$$A = \frac{-1}{RC} \qquad B = \frac{C_{op}}{C}$$
$$G = [G_1 G_2] \quad C = 1 \quad D = [0\;0\;0]$$

Here, R and C are the thermal resistance and capacitance of the building, respectively. The system time constant is $\tau = RC$. The HVAC input is discrete: $u = \{0{,}2.5\;kW\}$, and y is the measured indoor air temperature. We range the time constant from 22.2 hours to 225 hours in order to cover most practical HVAC scenarios. The models indexed in order along with their time constants that are obtained by varying their resistances and capacitances are shown in Table 1. For a step input of 2.5 kW, the indoor air temperatures obtained from all the considered HVAC models are shown in Figure 1. The disturbances considered are the external temperature and solar irradiance – $v(k) = \begin{bmatrix} v_1(k) \\ v_2(k) \end{bmatrix}$ – and are shown in Figure 2.

Table 1: System parameters for a range of HVAC models.

Model Index	R (°C/kW)	C (MJ/°C)	Time Constant (hr)
1	2	40	22.22
2	2	56	31.11
3	3	52	43.33
4	4	48	53.33
5	5	46	63.89
6	5	54	75
7	7	44	85.56
8	6	58	96.67
9	8	48	106.67
10	10	42	116.67
11	11	42	128.33
12	9	56	140
13	10	54	150
14	12	48	160
15	14	44	171.11
16	13	50	180.56
17	12	58	193.33
18	13	56	202.22
19	16	48	213.33
20	15	54	225

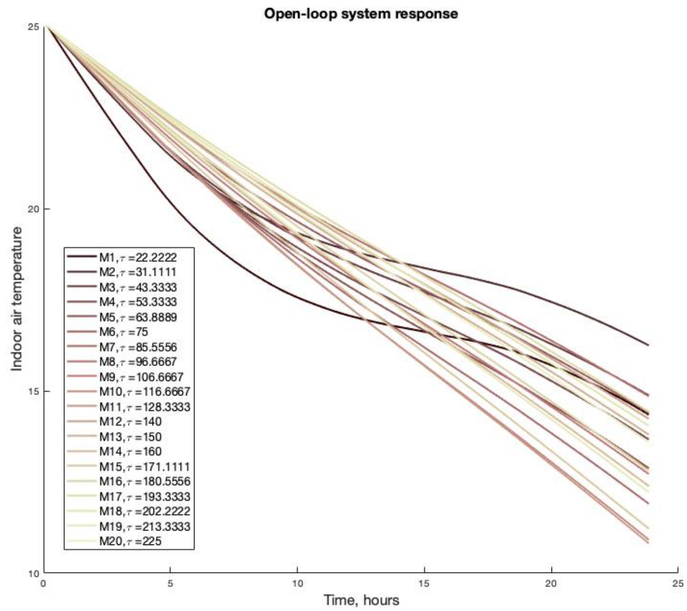

Figure 1. Temperature responses of 20 first-order HVAC models.

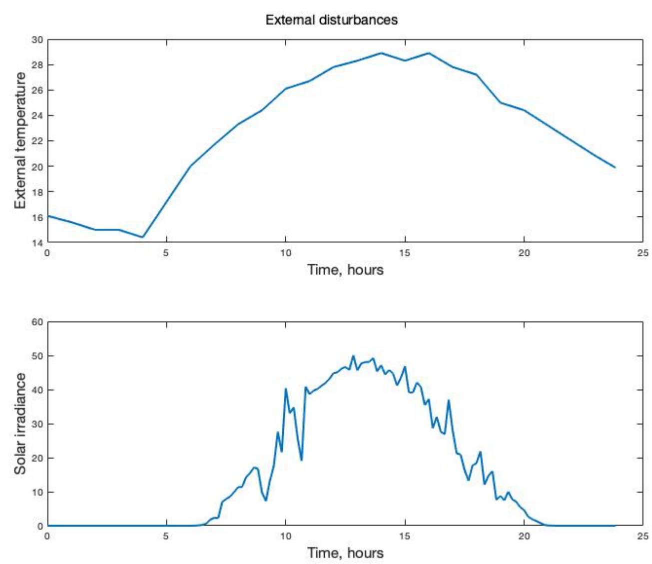

Figure 2. External disturbances considered in the HVAC models.

Having seen the system response for the rated power of 2.5 kW, we now observe the system for different input (rated) powers to gain more insight into the system dynamics. For the fastest model – M_1 in Figure 1, the temperature responses for a range of rated powers from 0 to $2.5\ kW$ are shown in Figure 3. As we can see, the system response is similar for inputs up to $300\ W$, and is almost the same as the HVAC being switched off. We can also clearly observe the inherent effect of the external disturbance in such cases.

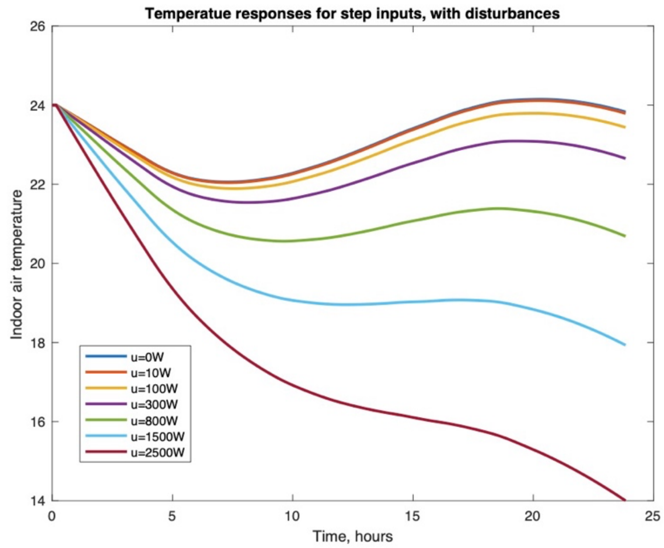

Figure 3. Output response of the first model M_1 for a range of HVAC input powers.

Continuous Control under Zero Time-Delay in Measurements

To establish a fair platform for analysis of MFC under time delays in measurements, we first establish a set of tuning parameters for each HVAC model without any time delay in measurements. Then we introduce time delays and observe the performance under the established tuning parameters.

To present a clear analysis, we consider three of the twenty models: M_1, M_{10}, M_{20} for the rest of the paper. In Figure 4 we show the temperature responses of the three models controlled using MFC without any time delay in the measurements. Alongside the temperature responses, we also show the corresponding control inputs and the state of the tuning parameters used for the models.

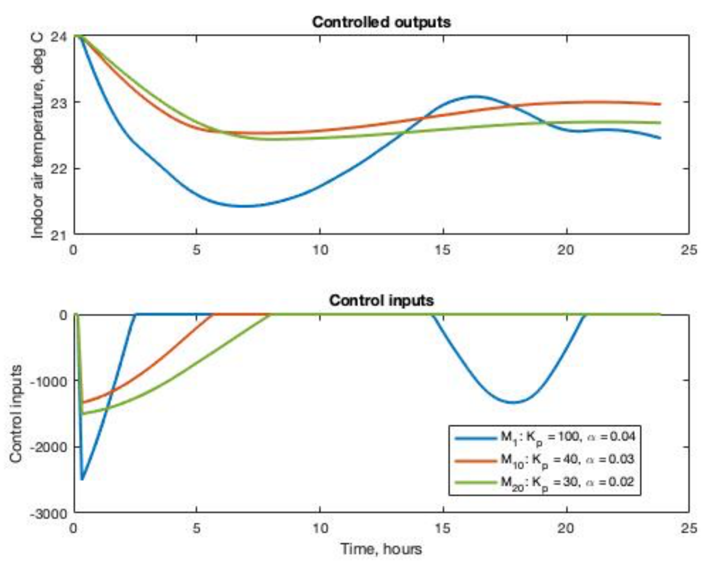

Figure 4. Baseline control of three HVAC models - performance under zero measurement time delays.

Control under Non-Zero Time-Delay in Measurements

With the MFC tuning parameters established under the absence of measurement time delays for the three considered models, we proceed to analyze their responses with the introduction of time delays in measurements. We also compare the responses obtained using MFC with an On-Off control strategy, or commonly known as thermostat control, which is defined to be ON except if the indoor air temperature hits the desired set-point. That is:

$$u(k+1) = \begin{Bmatrix} 2.5\ kW & if\ y(k) > y^* \\ 0 & otherwise \end{Bmatrix}$$

Note that the On-Off control strategy inherently leads to a discrete control input. Therefore, to maintain a fair comparison between On-Off and MFC, we round-off the control input from the MFC and accordingly switch on or off the HVAC. This results in the final HVAC power input resulting from the MFC strategy to be discrete, not continuous.

The sampling time considered is 10 minutes, and hence each time delay in a sample corresponds to 10 minutes. Accordingly, a measurement delay of 6 samples corresponds to one hour delay in measurements. We present the controlled temperature responses for the three models M_1, M_{10}, M_{20} under different measurement time delays in Figures 5-7. In each figure, along with the temperature responses, we also show the corresponding control inputs. We note here that the tuning parameters for MFC are the same as obtained under the absence of measurement time delays. Each figure considers one model, and in the subplot columns therein, it shows the comparison between On-Off and MFC. While the top row shows the indoor air temperatures obtained for different measurement time delays under the two control strategies, the bottom row shows their corresponding control inputs. For all the three models under a range of considered measurement time delays, as we can see, the MFC strategy is able to handle the time delays effectively and outperforms the On-Off strategy.

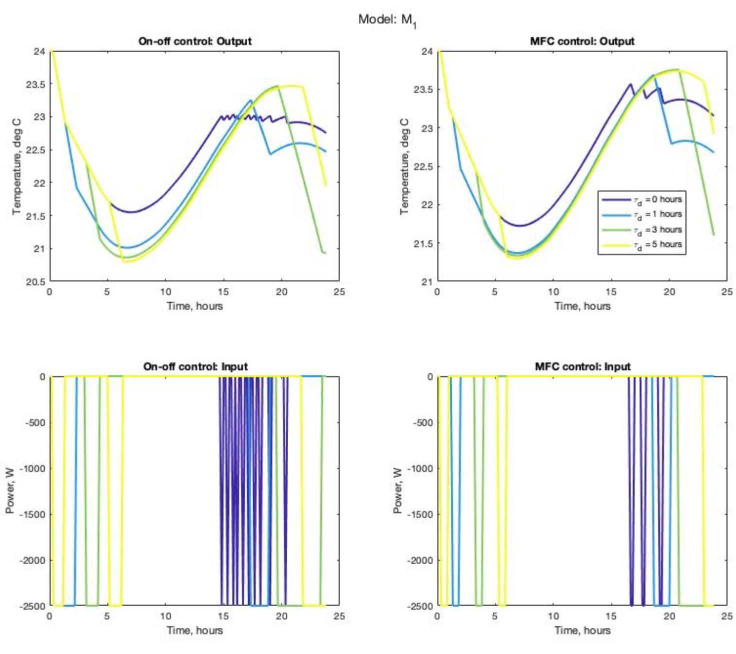

Figure 5. Comparison of On-off and MFC for Model-1 under different measurement time-delays. Top row: Indoor air temperatures. Bottom row: HVAC input states.

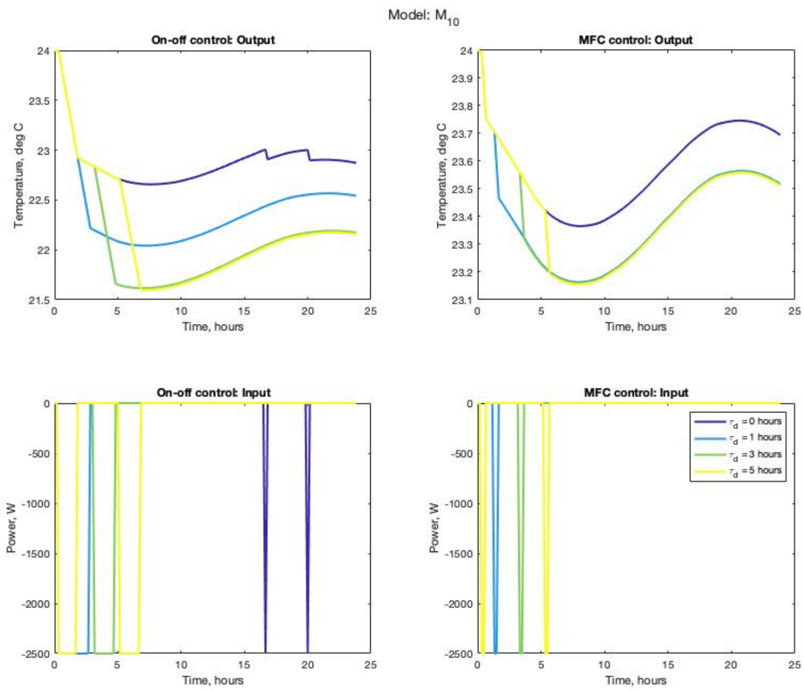

Figure 6. Comparison of On-off and MFC for Model-10 under different measurement time-delays. Top row: Indoor air temperatures. Bottom row: HVAC input states.

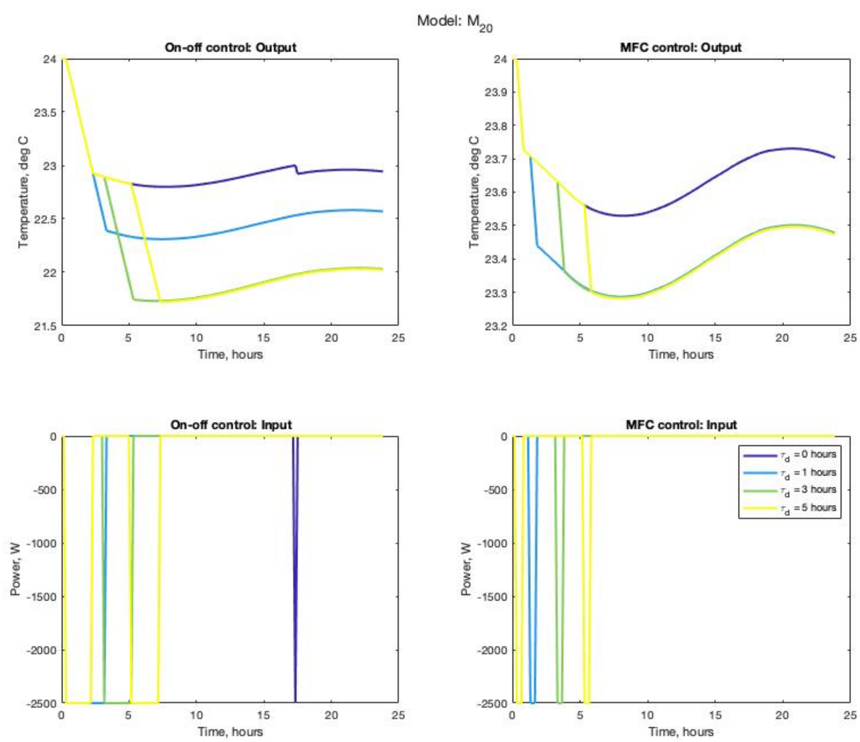

Figure 7. Comparison of On-off and MFC for Model-20 under different measurement time-delays. Top row: Indoor air temperatures. Bottom row: HVAC input states.

The results shown in Figures 5-7 are further analyzed through different metrics as shown in Table 2. For all the three models, we compare the two strategies – On-Off control and MFC – through their ability to maintain the desired temperature setpoint and through their power consumption. Accordingly, the first metric is the absolute mean deviation, which is the mean of the absolute difference between the measured temperature and the desired temperature setpoint. This error measurement metric is denoted e_{amd}. The second metric is the power consumption, which is the average power consumed, in kW, by the HVAC over a 24-hour period, denoted p_{avg}. As observed in Table 2, the power consumption using MFC is significantly less than the one for on-off control. Additionally, in most cases the deviation in indoor air temperature from the desired setpoint is also less than on-off control.

Table 2. Comfort satisfaction and power saving of on-off control and MFC for Models 1, 10, and 20.

Model Index	Time Delay (hr)	0		1		3		5	
		On-off	MFC	On-off	MFC	On-off	MFC	On-off	MFC
1	e_{amd}(°C)	0.5760	0.6006	0.9529	0.7507	1.0630	0.8202	0.9277	0.7854
1	$p_{avg}(kW)$	40	25	55	42.5	90	67.5	65	35
10	e_{amd}(°C)	0.2059	0.5780	0.685	0.3959	0.9753	0.4107	0.8993	0.4259
10	p_{avg} (kW)	27.5	5	37.5	10	47.5	10	47.5	10
20	e_{amd}(°C)	0.1529	0.6454	0.5499	0.4239	0.9806	0.4429	0.8975	0.4620
20	p_{avg} (kW)	32.5	7.5	45	15	62.5	15	62.5	15

Effect of Measurement Time-Delay in Power Allocation

Let $P(k)$ be the amount of power to be allocated by the central command among N different TCLs at time k. Let $u_i(k)$ and $y_i(k)$ be the "ideal" control input and the corresponding output of the i^{th} TCL at time k, and $P_i(k) \in \{0, p_r\}$ be the power consumed, where p_r is the rated power of the TCL, which is 2.5 kW in this study. The "ideal" control input refers to the control input computed from the local control method and would be supplied to the TCL had there been no power allocation constraint. However, in order to follow the reference power profile, the central command receives all the "ideal" control inputs and sends back power inputs to the TCLs such that the power allocation constraint is satisfied while deviating the least from the ideal requirements.

$$P(k) - \epsilon \leq \sum_{i=1}^{N} P_i(k) \leq P(k) + \epsilon$$

The central command maintains the power allocation constraint above in the following steps:

1. Compute the number of TCL units to be switched on as $n_{on} = \text{round}(\frac{P(k)}{p_r})$.
2. Use the "ideal" control inputs $u_i(k)$ to rank the TCLs – higher value reflects the urgency of the TCL to be switched on.
3. Set the top n_{on} TCLs' inputs to 1 (switch on) and rest to 0.
4. Communicate the modified control inputs back to the local controllers.

Note here that the central command employs the "ideal" control input from all the local controllers only to rank the loads in terms of the urgency in needing additional power. The number of units to be turned on at a certain time instant is only based on the available power at that time instant. Therefore, regardless of the state of the TCL output, only a pre-decided number of TCLs are turned on. The aspect that the measurement time-delay will affect certain units being wrongly turned on, and certain others being wrongly turned off. Therefore, we will observe the negative effects of the measurement time delays in the TCLs' temperature outputs deviating from their desired setpoints; however, the power allocation constraint will always be satisfied. Accordingly, if the power profile is feasible, then the chances of all TCLs' temperature outputs deviating the least from their desired setpoints is high.

The scale of the resulted data to present power allocation among 100 HVACs of three different models for a range of measurement time delays is too large to meaningfully present as visual graphs. Therefore, we present the power allocation results – temperature responses and power consumption – for M_1 with and without measurement time delays. Then, we present the rest of the large, resulted data in a table by analyzing it through different metrics.

Figures 8-10 shows the results of power allocation for M_1, where the considered time delays are 0 and 5 hours. Since the power consumption profile is the same for both the cases, we only show the power graph once. The metrics we consider for further analysis of the large-scale resulted data are absolute mean deviation and average number of switching. The former, error through absolute mean deviation denoted e_{amd}, is computed the same way as in the case of no power allocation. The latter is computed as follows. Each time an HVAC changes its state, from On to Off or vice versa, it is considered to have switched. The total number of switching of each HVAC, throughout the span of 24 hours, is then averaged to obtain the second metric – average number of switching per HVAC per day, denoted η_s. Like Table 2, the first entry in each cell corresponds to On-Off control and the second entry corresponds to the MFC.

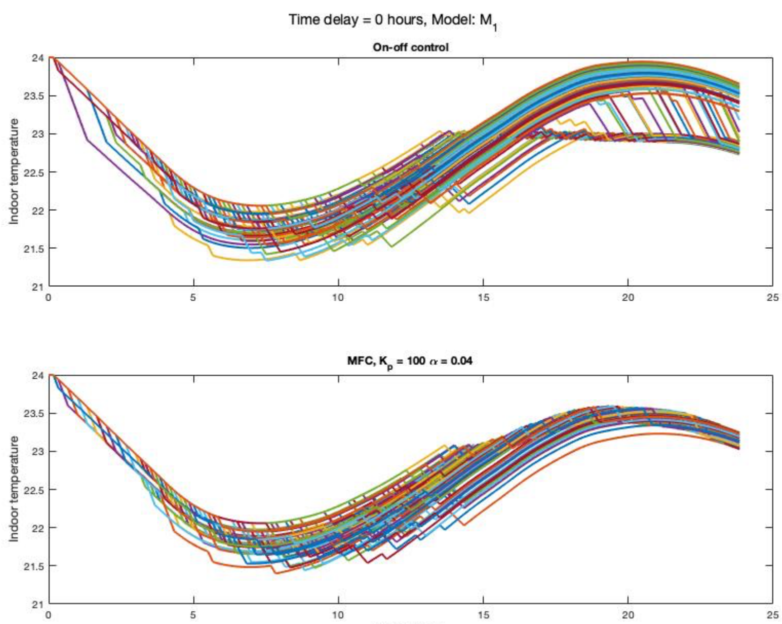

Figure 8. Temperature responses of 100 HVACs of Model-1 obtained with power allocation constraint and no time-delay in measurements.

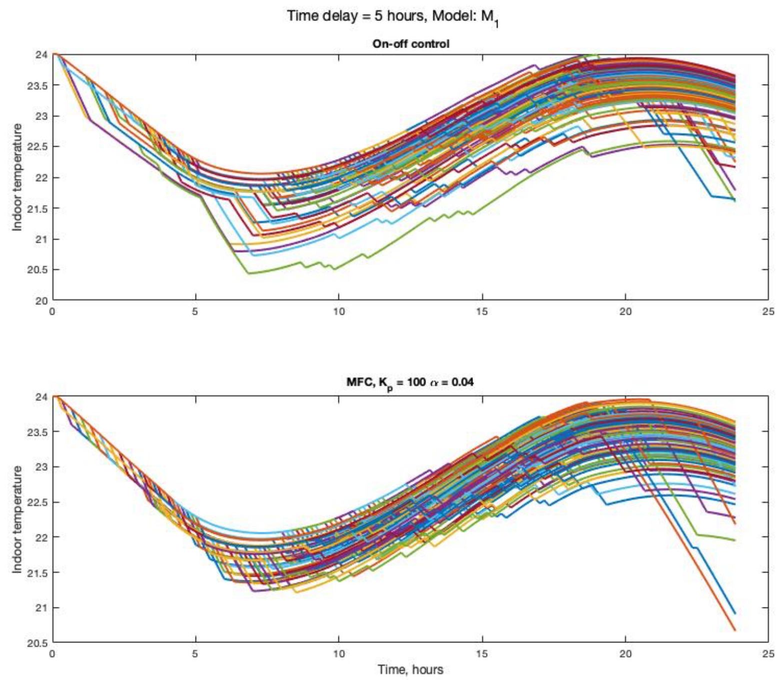

Figure 9. Temperature responses of 100 HVACs of Model-1 obtained with power allocation constraint and a measurement time-delay of 5 hours.

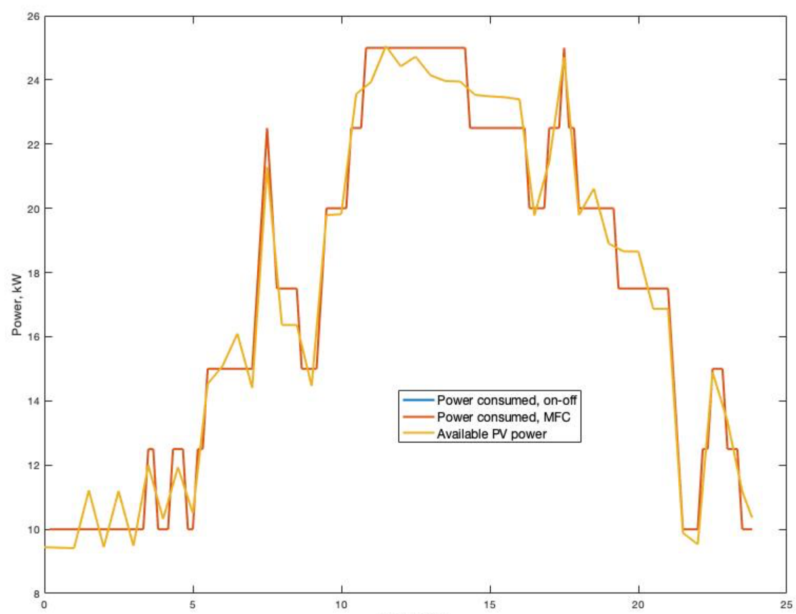

Figure 10. Power tracking of the reference (available) power by the central command, using on-off control and MFC.

Table 3. Comfort satisfaction and HVAC switching under power allocation constraint using on-off control and MFC for Models 1, 10, and 20.

Model Index	Time Delay (hr)	0		1		3		5	
		on-off	MFC	on-off	MFC	on-off	MFC	on-off	MFC
1	e_{amd}(°C)	0.5969	0.5791	0.6416	0.5909	0.6245	0.6162	0.6152	0.6069
1	η_s	15.68	13.64	10.58	11.16	12.02	12.36	13.06	13.24
10	e_{amd}(°C)	0.3754	0.3221	0.6330	0.3909	0.8524	0.6428	0.8897	0.5947
10	η_s	8.34	9.84	1.76	3.02	1.28	2.72	1.32	3.36
20	e_{amd}(°C)	0.5427	0.5075	0.7289	0.5164	0.9026	0.6959	0.9429	0.6954
20	η_s	4.86	9.8	1.38	3.02	1.2	2.76	1.08	3.36

Overall, mean deviation in indoor air temperatures is less using MFC than using on-off control. However, the switching rate is slightly higher in MFC in most cases.

Conclusion

Despite the introduction of time delays in measurements, we observe that the power allocation constraint is always satisfied. This is due to the framework of the algorithm embedding the power allocation as a hard constraint. When there is a time delay in measurements, the local controller – on-off or MFC – does not have the latest (and hence the most accurate) measurement to operate on. This leads to certain deviations from the desired temperature setpoint. However, as we have observed the MFC strategy is nonetheless robust to measurement time delays for at least up to 5 hours, which is practically a sufficient time to correct the faults causing the delays.

Acknowledgment

This material is based upon work supported by the U.S. Department of Energy, Office of Energy Efficiency and Renewable Energy, Building Technologies Office. This manuscript has been authored by UT-Battelle, LLC under Contract No. DE-AC05-00OR22725 with the U.S. Department of Energy. The United States Government retains and the publisher, by accepting the article for publication, acknowledges that the United States Government retains a non-exclusive, paid-up, irrevocable, world-wide license to publish or reproduce the published form of this manuscript, or allow others to do so, for United States Government purposes. The Department of Energy will provide public access to these results of federally sponsored research in accordance with the DOE Public Access Plan (http://energy.gov/downloads/doe-public-access-plan).

References

Fliess, M, and Join, C. 2013. “Model-free control”, *International Journal of Control,* 86:12, 2228-2252.

Hayat, M, Dhakal, S, Abdallah, C, Birdwell, J, Chiasson, J. 2003. “Dynamic Time Delay Models for Load Balancing Part II: A Stochastic Analysis of the Effect of Delay Uncertainty” *CNRS-NSF Workshop: Advances in Control of Time-Delay Systems.*

Jama, M. A., Noura, H., Wahyudie, A., & Assi, A. 2015. Enhancing the performance of heaving wave energy converters using model-free control approach. *Renewable Energy*, *83*, 931-941.

Lafont, F., Balmat, J. F., Pessel, N., & Fliess, M. 201. A model-free control strategy for an experimental greenhouse with an application to fault accommodation. Computers and Electronics in Agriculture, 110, 139-149.

MohammadRidha, T., Aït-Ahmed, M., Chaillous, L., Krempf, M., Guilhem, I., Poirier, J. Y., & Moog, C. H. (2017). Model free iPID control for glycemia regulation of type-1 diabetes. *IEEE Transactions on Biomedical Engineering*, *65*(1), 199-206.

Nilsson, J. 1998. “Real-Time Control Systems with Delays”.

Oriz, L, González, J, Gutierrez, L, Llanes-Santiago, O. 2020. “A review on control and fault-tolerant control systems of AC/DC microgrids”, *Heliyon*. Volume 6, Issue 8.

Park, C, Yang, T. 2017 “Comparative review and discussion on P2P electricity trading”, *Energy Procedia,* Volume 128, Pages 3-9.

Telsang, B, Amasayali, K, Chen, Y, Olama, M, Djouadi, S. 2021. “Power allocation by load aggregator with heterogeneous loads using weighted projection”. *Energy and Buildings*, Volume 244.

Telsang, B, Djouadi, S, Olama, M, Kuruganti, T, Dong, J, Xue, Y. 2018. "Model-free Control of Building HVAC Systems to Accommodate Solar photovoltaicEnergy," *9th IEEE International Symposium on Power Electronics for Distributed Generation Systems (PEDG)*, pp. 1-7.